Zhongguo Kuangye Daxue Xuebao
Journal of China University of Mining and Technology

A Semi-System Approach to Determine the EHL Model over the Contact Length and Its Effect in Helical Gear Pair

Ashutosh Kumar*
Department of Mechanical Engineering, D. Y. Patil University, Ambi, Pune, 410506, Maharashtra, India
*Corresponding author

Kiran More
Department of Mechanical Engineering, D. Y. Patil University, Ambi, Pune, 410506, Maharashtra, India

Abstract

Helical gears because of their low noise operation and better efficiency are one of the best choices for various industries wherever they are using parallel shaft gear drive. These gears normally operate in elastohydrodynamic lubrication (EHL) condition to transfer high torque. In such scenario the lube film thickness plays a very critical role in the fatigue life of the gears. It is important to know the contact pressure, lube film thickness and pattern of oil film pressure at critical points of load transmission. This research work is all about determination of lube film thickness, contact pressure and oil film pressure at all concern contact points on contact line.

To start with the research after analysing the past work done the critical points are being calculated as per AGMA 925 followed by detailed analysis on these points to establish their validity and significance. Critical Points are discussed. Reynolds equation is used to establish the methodology of calculating the lube film thickness with numerical methodology concept for elastic deformation. A noble method of calculating the lube film thickness by following the methodology as discussed in Python is used here. The contact stress model generated in the Python is reviewed for sample example with analytical result to find its accuracy. Lube film thickness is calculated in line with AGMA 925 via Kissoft and each point pressure with lube film pattern is calculated by the Python tool in this research work. Finally, the developed software is also reviewed with historic example data and was found satisfactory.

Keywords

EHL, Contact line, KISSOFT, Python

Nomenclature		
Symbol	**Description**	**Units**
bH	Hertz dimension in y direction	mm
d	surface deformation	mm
$d_{1,2}$	Pitch Circle diameter of Pinion and wheel	mm
E_r	Reduced modulus of elasticity	N/mm^2
$E_{1,2}$	Young modulus of elasticity, surface 1 & 2	N/mm^2
h	Film thickness	mm
G_M	Material Parameter	-
P	Pressure	N/mm^2
$R_{1,2}$	Radius of curvature, surface 1,2	mm
$S_{GF,Y}$	Load sliding parameter	-
U_y	Speed Parameter	-
W_Y	Load parameter	-
$r_{a1,2}$	Addendum circle radius pinion and wheel	mm
$r_{b1,2}$	Base circle radius pinion and wheel	mm
$r_{tip1,2}$	Tip radius pinion and wheel	mm
$V_{r1,2}$	Rolling Velocity of pinion and gear	m/s
$u_{1,2}$	Velocity of surfaces 1,2 in y direction	m/s
v_s	Sliding Velocity	m/s
v_e	Entraining Velocity	m/s
$v_{ss1,2}$	Specific sliding velocity Pinion and Gear	m/s
x	Coordinate in the entertainment direction	-

y	Coordinate transverse to the entertainment direction	-
α_0	Pressure viscosity coefficient	Pa^{-1}
β_b	Base helix angle	degree
γ_0	Density pressure coefficient	Pa^{-1}
η	Absolute viscosity	Pa.s
η_0	Absolute viscosity at reference temperature	Pa.s
α_n	Normal Pressure angle	degree
λ_{0n}	Density Pressure coefficient	-
ρ	Density	N/mm^3
ρ_0	Density at reference pressure	N/mm^3
$\rho_{1,2}$	Radius of Curvature of pinion and gear	mm
ρ_n	Normal radius of Curvature of (relative)	mm
$\nu_{1,2}$	Poisson's ratio of pinion and gear	-
ζ	Slide to roll ratio	-
$\omega_{p,g}$	Angular velocity of Pinion and Gear	rpm

1. Introduction

Gears being positive drive play a critical role in torque transmission over a wide distance range with high efficiency for a variety of torque levels. To ensure the continuity of its operation it is important to provide it adequate design environment suitable to it. Lubrication comes in action as one of the critical parameters. Significance of lubricant becomes more critical in between the contact of the gear pair where high torque transmission occurs. In such condition, it is important to determine the critical torque transmission points. At these points there should be sufficient lubricant film thickness that it can maintain the desired gap in between the gear pair while transmitting the torque. As to summarise the steps followed in this research will start from previous research study work, followed by critical point determination, EHL step creation in python, Lube film thickness determined at critical points with detail analysis and EHL presentation at each point by the new method developed in this research work.

1.1 Previous Research Work

EHL refers to the state of thin film of lubricant in between two contacting non conformal surfaces. It is formed because of three major effects as hydrodynamic lubrication effect, elastic deflection in between two contacting bodies and the pressure viscosity variation in lubricant while entering the contacting zone. Dowson & Higginson released the first paper in 1959 as a solution of the EHL problem for a cylinder rolling on a plane. Later in line various other research works were done as detailed below.

H. Spikes et al. [1] Analysed the various rheological model to elaborate the working of thin films while rolling sliding, and elastohydrodynamic contacts. Researcher has reviewed all the past research work related to thin film friction under high pressure and associated conflicts as of now. Based on the work it was concluded that friction can be controlled by viscosity response, low specific sliding and corresponding shear thinning response. To come to this conclusion various curves were plotted related to strain rate, specific speed, pressure, and viscosity.

G E Morales et al. [2] worked on a review of EHL. In this work smooth surface was considered first for the analytical solution. Thermal effect on account of rolling frictions was considered in terms of lubricant temperature change. Thermal consideration spanned on the surface also along with fluid. Entering and existing pressure of the lubricant were calculated with transient condition. In all the analysis linear fracture mechanics concepts was considered. Various curves were plotted to establish the relationship between various parameters. It was found that the simple methods can also be used to get the accurate solution.

A study on the numerical solution of the isothermal Elastohydrodynamic Lubrication (EHL) for elliptical-shaped point contacts was conducted by D. Dowson et al. [3]. In this work, he adjusted the approaching geometries' arrangement to alter the elliptical contact's asperity ratio. The work began with a point contact to a line contact problem involving a ball and plate contact. The suggested approach and the Archard-Cowing formula were compared. The findings were also applied to further tests.

Researchers T G Huges et al. [4] studied the connection of the elastohydrodynamic issue. Here, the effort was to pair all of the Elastohydrodynamic Lubrication (EHL) equations in order to characterise the EHL problem's line contact. The goal was to provide a numerical solution for the analysis of rough surface contact and thin film, both of which are prevalent in gears. It was discovered that the surface's deformation behaviour had the most influence. It was discovered that full coupling—as opposed to partial coupling—is desirable for line contact problems.

Using the differential deflection approach, T G Huges et al. [5] calculated the deflection caused by pressure acting on a semi-infinite body. This is easily adaptable to the line contact Elastohydrodynamic Lubrication (EHL) issue. Instead of employing an explicit approach, the differential deflection method describes the deflection in a distributed implicit manner. Although the total process time was less than in the past, the procedure yields outcomes that are remarkably similar to previous findings with other methods.

A computational technique for resolving point contact issues in elastohydrodynamics under moderate stress was presented by H P Evans et al. [6] Issue with lubrication in isothermal environments. The elastic deformation equation was created using the fundamental equation of deformation. The finite difference grid approach was used with an iterative solution

process. Both exponential and power law viscosity-pressure relationships for lubricants were studied numerically at a variety of loads and speeds. Additionally, a numerical solution flow diagram was created. When a profilometer was used to validate the surface's roughness, results were produced for moving rough surfaces. For smooth surfaces, an analogous exercise was also conducted. This exercise was carried out using a very low lambda value for a range of slide to roll ratio values.

The Laplacian of deflection of a semi-infinite body exposed to pressure loading was assessed by H P Evans et al. [7]. Both line and point contacts were taken into account in this investigation. From the fundamental equation, an expression for the deflection due to line contact was created. The Laplacian equation for the deflection at a point was also constructed in a similar manner. Plotting several charts was done after evaluating the numerical solutions to the line contact problem and the point contact problem. A hertzian pressure distribution was used to confirm the method's accuracy for both point and line contact.

The helical gear's film parameter and friction coefficient were examined by Lin Han et al. [8] after surface roughness and load change were taken into account. Here, a load distribution model using finite element analysis and point-by-point calculations of the geometric and kinematic parameters was used. The action plane, which also made use of the load sharing notion, was taken into consideration. The impact of transmitted load, rotational speed, and surface roughness on friction coefficient was examined and discussed. Conclusion: Rougher surfaces have a higher friction coefficient. Increasing pinion speed might hasten the time it takes for lubrication to move from boundary to mixed conditions. The applied load immediately affects the friction coefficient.

A report on the impact of asperities in elastohydrodynamic lubrication (EHL) was given by M. Kaneta et al. [9]. In the experiment, rough surfaces under point contact in lubrication were studied using optical profilometry. To rotate the ball in the race, the traction force was transferred through the EHL film in the experimental approach. A portion of the ball's surface has splotchy asperities. Chromium was the substance spluttering. There was a set weight of 4 kg, which corresponded to a specific Hertz pressure of.55 Gpa. The experiment revealed some intriguing results, one of which was that the asperities behaved differently in rolling and sliding motion. Sliding was complicated because the film thickness was too low.

The transient mixed Elastohydrodynamic lubrication (EHL) model for spur gears was the focus of S. Li et al.'s study [10]. The lubricant's state was regarded as non-Newtonian. The EHL model used in this study was intended to continually track the tooth pair contact from root to tip and was applicable to spur gears. The distribution of normal tooth force along the action line was predicted using the gear load distribution technique. Using the EHL model, the minimum change in film thickness over the contact line's surface was ascertained.

The assessment of film thickness in elastohydrodynamically lubricated elliptic contacts was the focus of Nijenbanning et al.'s study [11]. For elliptical contact scenarios, the circular contact solver was expanded. To verify the novel expanded model for elliptical contact, existing literature was consulted. It is demonstrated that both the pressure and the film thickness can be precisely predicted using the line of contact analysis. Additionally, a formula for estimating the minimum and centre film thickness is given. The formula is applicable to all load conditions and takes asymptotic behaviour into account.

A. P. Ranger [12] came up with a solution to the point contact elastohydrodynamic issue. Two surfaces are thought to be in touch, one of which is an elastic plane and the other an elastic sphere. On the elastic plane, the elastic sphere is rolling. Consistent operation with an isothermal film is regarded as the operating condition. Together with simultaneously calculating the elasticity equation and Reynold's equation, the pressure viscosity exponential characteristic is taken into account. Matrix of deformation deemed sufficiently compact. Multiple regression analysis was used to analyse the data in order to broaden the solution. The outcome was quite comparable to data that had been published.

Theoretical investigation of the isothermal electrohydrodynamic lubrication (EHL) of concentrated contacts was conducted by R.J. Chittenden et al. [13]. He calculated seventy-two new EHL solutions in all, which were reported in two articles. This paper discusses thirty-four of them. In this article, the analysis took into account the contact ellipse's aspect ratio. Basic equations were used to formulate analytically. The EHL equation was taken into consideration along with elastic deformation and lubricant characteristics. For the same purpose, a computer chart and a computer programme were created.

X. Ai et al. [14] used a multigrid approach to evaluate transient Elastohydrodynamic lubrication (EHL) study for line contacts with observed surface roughness. The surface roughness effect is included in the film thickness equation, whereas the Reynolds equation served as the controlling formula. Pressure-Viscosity Relation: A modified two-slope exponential model was taken into consideration. The Reynolds equation was discretized using Euler's stability consideration. It was discovered that surface roughness causes a fleeting impact. Pressure fluctuation rises in tandem with the relative speed increase between the contacting surfaces.

Using two distinct lubricants in a test rig, Xiaojing et al. [15] examined the link between micropitting and tribology with varying geometric slide to roll ratios. Using an optical microscope, the degree of micropitting was determined. When doing this investigation, humidity was taken into account as well. The study's findings indicate a link between humidity and the slide-to-roll ratio, with higher humidity corresponding to increased wear.

A case study of the ISO/TS 6336-22 micropitting computation was evaluated by O.Robin et al. [16]. An analysis of the micropitting load capacity of external spur gear sets through testing is described in ISO/TS 6336-22. The safety

factor against micropitting, known as the lambda ratio, is determined by calculating the ratio between the minimum film thickness and micropitting, and taking into account the link between the two. A case analysis was carried out. Since micropitting was anticipated on the tooth's surface, it was determined that surface roughness and film thickness alone were insufficient to predict micropitting.

The spur gear tooth profile modification approach for reducing micropitting was examined by X. Xu et al. [17]. By meshing the gear teeth, Hertz contact stress spots on the tooth flank were shown. Here, the tip relief process is applied, and related mathematical equations were created. Hertz stresses were linked to micropitting, and as a result of changing the tooth's curvature, the hertz stress values at crucial locations decreased. Taking into account the decrease in micropitting.

Using the Elastohydrodunamic lubrication model, A.C. Redlich et al. [18] examined the mixed lubrication regime. Point interactions were taken into account in the in-depth examination. For this regime, the contact and lubricant film pressures were computed and displayed. The image also took surface roughness into account, therefore iterations were needed to answer the equations. A multigrid technique was employed to address the issue. The analysis was expanded upon to investigate the impact of various rough surfaces at various velocities. Pure sliding conditions to various surface velocities are included in the velocities.

The multigrid method for resolving the Elastohydrodynamic lubrication model was developed by C.E. Goodyer et al. [19]. The multigrid method has shown to be highly helpful because the EHL model requires a large iteration count to solve. For stable issues, the equation's convergence to produce excellent results was seen. This study essentially described how the equations were convergent to the solution under both steady-state and transient situations.

A. Jolkin et al. [20] used the optical approach to estimate the thickness of the elastohydrodynamic lubrication film as well as the oil film thickness with a ball and disc setup. In the experiments, synthetic polyyalphaolefin oil was utilised. In parallel, the pressure envelope was compared and the oil film thickness was calculated numerically. For the specified pressure and temperature circumstances, both findings demonstrated good agreement.

The computational model of elastohydrodynamic lubrication for involute spur gears was presented by S. Khalilarya et al. [21]. The lubricant was thought to be according to Newton's law in order to prepare the model. The line of contact was used for the whole analysis. The gear tooth bending, shearing, compression, and tilting activities were taken into consideration while creating the numerical model, and the results were highly consistent with both analytical and experimental findings. The findings of this experiment were made available for a range of lubricant film thickness values, pressure distribution values, and pressure envelope values. K. Chen et al.'s analysis [22] looked at the numerical solution between two surfaces with high roughness values but varied levels of roughness. To ascertain the impact, several coarse particles were also inserted in between these surfaces. The film pressure distribution was calculated using Reynold's equation. The results were impacted by both the third particles and the roughness. For the whole study, non-dimensional characteristics were taken into account. After analysing a number of circumstances, it was discovered that the rough surface and the particle existence between them were the reasons why the oil thickness was rapidly decreasing.

K. K. Manesh et al. [23] Worked on roughness of surfaces in 3 dimensions. He used 2D digital filter method for the regeneration of numerical process. He also generated 3 dimensional surfaces to deal with engineering problems. Researcher found that this methodology of generating numerical method was yielding good results as compared to other methods for his problem case. This was also proven by matching with the 3d model generated by him and the numerical model.

Francesc P. R. et al. [24] Developed the rough surface generation technique by using power spectrum method. Statistical methodologies were used along with engineering inferences. In the research work non gaussian surfaces were shown. It was observed that a good result can be developed by giving the least effort. MATLAB codes were also developed to show the results. Overall, the techniques used here has opened a new direction to work on tribological issues.

Ulrich Kisling [25] worked on micropitiing calculation by considering ISO and AGMA methods. He worked on all the parameters responsible for micropitting like geometry parameters, surface finish, lubricant, load parameters, speed parameters etc. All these parameters are equally responsible for the EHL model development and their effects as well. The performed mathematical calculation was done in Kissoft and the findings were very much useful to understand the minimum lube film thickness occurring and their effects on surface fatigue.

Pawlus P. et al. [26] reviewed the methodology of surface topography generation. This work helped in corelating the machined surface property as well. Various past methods used for such topology were studied al together and at last tribological topology was developed.

D. Dowson et al. [28] worked on the very early and basic methodology used in EHL model. Opti9cal methodologies were used, and the previous works were compared. A through detailing was done in the development of the required formed equation which is needed for the analysis. Shear thinning concept was discussed and various graphs were plotted to release the conclusion.

Quentin A. et al. [29] performed the research work on the low load EHL model and also comparted the data with high load models. The work was not contributing directly to this research work however the methodology to deal with EHL model with fairly soft material was a good finding to give direction to this research work.

MG Wu et al. [30] concentrated the work on the development of EHL Model in the mixed lubrication condition. The work was performed for cylindrical spur gear. Idea was to know the effect of friction on the life of the gears by developing the EHL model and this analysis was performed on five critical points. Numerical method was developed and cross checked with Dowson's method to ensure its accuracy.

Quentin A. et al. [31] continued his research soft EHL model and comparted the data with high load models. He worked on sliding parts having the textured surface. He used his past research concept and applied here. The surface model was discretised and the convergence of discretization matrix was given atmost important to yield the result.

Ferdinand S. et al. [32] performed the research of high load internal gears and coined this has hard EHL. A good definition where the gear pair was loaded to the maximum possible extent and thus creating the EHL condition. Overall, the concepts here was to identify and detail the effects in internal gears.

Yangyi X. et al. [33] worked on EHL model work for the systems where numerous coatings are provided to avoid any surface distress. The concept here was more on heavily loaded contact points. Finite element analysis was initially considered and later on EHL model was developed. An initiative here was to consider the stiffness of the coating surfaces. A methodology was developed to ensure the surface damage process.

Yuko H. et al. [34] analysed the EHL model for sliding and contact point surfaces. By considering the very basic form the base equations were used and then the development of EHL model was done. More concern here was related to the oil film performance in terms of its rheological properties.

Zhaoqiang W. et al. [35] worked on sliding and contact point for the development of EHL model. Piton pump and Port plate pair were considered here. All the lubricant properties which are responsible for the load transmission were considered as a part of this work. It was found that the deformation in the oil film is responsible for oil leakage.

Chunxing G. et al. [36] performed the work on the adding of fluid and structural deformation equations with the addition of cavitation effect and material deformation. Two different methods were used to continue the research work. A new methodology was developed to get the desired solution of EHL model. The results were cross checked with past work.

Hai Chao L. et al. [37] identified the relevance of shear stress contribution and shear rate contribution to the EHL model. A non-Newtonian model was developed by considering all thee prementioned terms to get the desired solution. Rolling and sliding were the important parameter during the analysis. A 2d model was generated having transient nature. The methodology hereby found was very useful in bearings and gears.

Outcome of Literature Survey
The findings are depicted as below:
- ➢ A comprehensive research database is available to facilitate the development of the Elastohydrodynamic Lubrication (EHL) equation
- ➢ Diverse studies present various methodologies for addressing EHL problems.
- ➢ For the analysis of EHL in point, circular, and elliptical contacts, reliable techniques are available.
- ➢ Abundant data is accessible for the analysis of EHL in spur gear contacts.
- ➢ The contact line is recognized as the focal area for EHL analysis.
- ➢ Multiple papers offer a method to transform relations used for circular contact points to elliptical contact points.
- ➢ Several papers provide detailed explanations of practical methods for the experimental determination of fluid film thickness, with many of them being widely utilized.
- ➢ However, there is a limited availability of data pertaining to EHL analysis in the contact lines of helical gears.

1.2 Problem Definition
This research focuses on the analysis of a helical gear pair, specifically involving a pinion with 24 teeth and a gear with 97 teeth. The helix angle is set at 16.195 degrees, and the pressure angle is 20 degrees. The pinion, rotating at 55 rpm, is subjected to an input power of 0.5 horsepower. The objective of the study is to develop an Elastohydrodynamic Lubrication (EHL) model under isothermal conditions, considering a Newtonian lubricant. The methodology employed in this research aims to ascertain lube film pressure, thickness across contact points, and various influencing parameters.

1.3 Determination of Important Point Of Contact Line
For an external gear pair, Figure 1 shows several diameters and positions on the contact line in the transverse direction. CJ distances are calculated along the line of action starting at the pinion's interference point. The pinion's start of active profile (SAP) is indicated by distance CA, while its end of active profile (EAP) is shown by distance CE. The positions of a single tooth pair contact's lowest and highest points (LPSTC and HPSTC), respectively, are shown by the distances CB and CD. Distance CC represents the operational pitch point, while distance CF indicates the distance between the base circles along the action's path.

$$u = \frac{z_2}{z_1} \quad\text{... (1)}$$

$$C_F = a_w \sin(\alpha_{wt}) \quad \text{...} \quad (2)$$

$$C_A = C_F - \sqrt{(r_{a2}^2 - r_{b2}^2)} \quad \text{...} \quad (3)$$
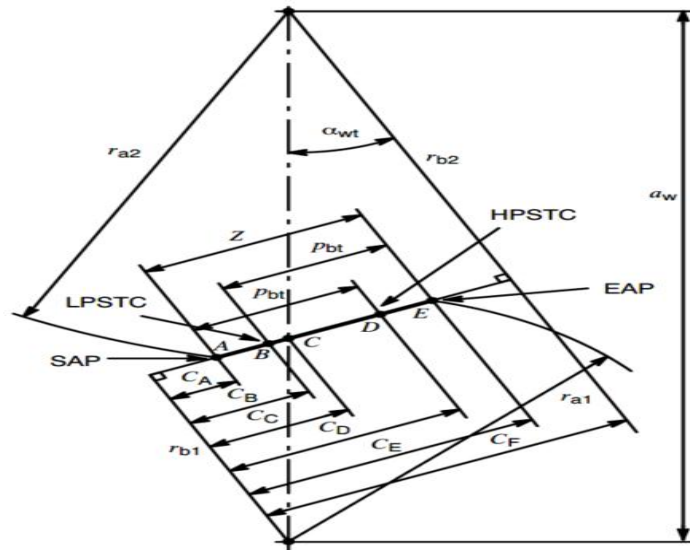
Fig. 1 Distances along the line of action for external gears

$$C_C = \frac{C_F}{u+1} \quad \text{...} \quad (4)$$

$$C_D = C_A + p_{bt} \quad \text{...} \quad (5)$$

$$C_E = \sqrt{(r_{a1}^2 - r_{b1}^2)} \quad \text{...} \quad (6)$$

$$p_{bt} = \frac{2\pi r_{b1}}{z_1} \quad \text{...} \quad (7)$$

$$C_B = C_E - p_{bt} \quad \text{...} \quad (8)$$

$$Z = C_E - C_A \quad \text{...} \quad (9)$$

Following the determination of various points along the line of contact, the subsequent step involves the computation of roll angles concerning the previously calculated points on the line of contact. This calculation can be expressed as:

$$\zeta_j = \frac{C_J}{r_{b1}} \quad \text{...} \quad (10)$$

Where,

J = A, B, C, D, E.

1.4 Contact Geometry
Gear pair in contact can be represented by a concept of equivalent radius [1] as shown in Equation -11.

$$\frac{1}{R'} = \frac{1}{R_1'} + \frac{1}{R_2'} \quad \text{...} \quad (11)$$
$$R_1' = r_{b1} \tan\alpha + s \quad \text{...} \quad (12)$$

$$R_2' = r_{b2} \tan\alpha - s \quad \text{..} \quad (13)$$

Where s is the distance of the point of contact from the pitch point. By following the equations 1-13 the values calculated are tabulated in Table-1

1.5 EHL Equation
The Elastohydrodynamic Lubrication (EHL) equation comprises two fundamental components: one derived from elasticity theory, addressing deformations, and the other from fluid film hydrodynamic equations. These components must

be coupled to yield the necessary results. The methodology adopted in this study employs a semi-system approach, wherein the solution to both the hydrodynamics equation and elastic deformation is integrated. This approach, commonly known as weak coupling, involves an iterative solving method for each equation, ensuring the attainment of the desired level of accuracy.

- *Pressure Distribution*

Two-dimensional Reynolds equation [12] is given as:

$$\frac{\partial}{\partial x}\left(h^3 \frac{\partial p}{\partial x}\right) + \frac{\partial}{\partial y}\left(h^3 \frac{\partial p}{\partial y}\right) = 6\eta\left(u \frac{\partial h}{\partial x}\right) \dots\dots\dots\dots\dots\dots\dots\dots\dots (14)$$

where,

$$u = \frac{u_1 + u_2}{2}$$

It is difficult to solve the above partial differential equation analytically and hence numerical approach is used here. Numerical method comes with numerical error and to reduce is non-dimensional approach for variables [11] is used often. Non -dimensional parameters are used as below:

$$\bar{x} = \frac{x}{X}, \bar{Y} = \frac{y}{Y}, \bar{h} = \frac{h}{C}$$

After submitting the above values in Equation -14 we get:

$$\frac{\partial}{\partial \bar{x}}\left(\bar{h}^3 \frac{\partial \bar{p}}{\partial \bar{x}}\right) + \frac{X^2}{Y^2}\frac{\partial}{\partial y}\left(\bar{h}^3 \frac{\partial \bar{p}}{\partial \bar{y}}\right) = \left(\frac{C}{X}\frac{\partial \bar{h}}{\partial \bar{x}}\right) \dots\dots\dots\dots\dots\dots\dots\dots\dots (15)$$

As X and Y are the two directions then we can use the concept of long and short bearing to optimize the calculation results and steps.

- *Discretization Method*

In order to obtain a solution for Equation 15, the contact surface must undergo discretization into a specified number of nodes, as depicted in Figure 2. This discretization process involves employing rectangular control volumes centered around each node, where the dimensions of the control volume are denoted as Δx and Δy. Figure 2 visually represents a singular control volume utilized to characterize the Poiseuille term for node i, j. This term encapsulates the flow in both the x and y directions induced by the pressure gradient, as articulated through a Taylor series.
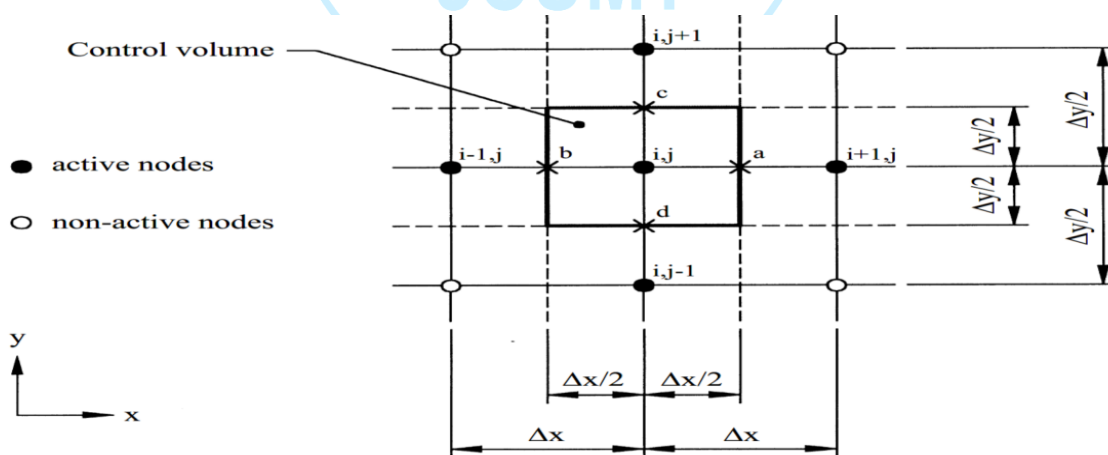

Fig. 2 Discretization of surface

$$\frac{\partial \bar{p}_{i,j}}{\partial \bar{x}} = \frac{\bar{p}_{i+1,j} - \bar{p}_{i-1,j}}{2\Delta \bar{x}} \dots\dots\dots\dots\dots\dots\dots\dots\dots\dots (16)$$

$$\frac{\partial}{\partial \bar{x}}\left(\frac{\partial \bar{p}_{i,j}}{\partial \bar{x}}\right) = \frac{\bar{p}_{i+1,j} - 2\bar{p}_{i,j} + \bar{p}_{i-1,j}}{(\Delta \bar{x})^2} \dots\dots\dots\dots\dots\dots\dots\dots\dots (17)$$

Using the Taylor series approximation, we will get:

$$\frac{\partial}{\partial \bar{x}}\left(h^3 \frac{\partial \bar{p}}{\partial \bar{x}}\right) = \frac{\bar{h}^3_{i+0.5,j}*\bar{p}_{i+1,j} + \bar{h}^3_{i-0.5,j}*\bar{p}_{i-1,j} - \left(\bar{h}^3_{i+0.5,j} + \bar{h}^3_{i-0.5,j}\right)*\bar{p}_{i,j}}{(\Delta \bar{x})^2} \dots\dots\dots\dots (18)$$

Similarly:

$$\frac{\partial}{\partial \bar{y}}\left(h^3 \frac{\partial \bar{p}}{\partial \bar{y}}\right) = \frac{\bar{h}_{i,j+0.5}^3 * \bar{p}_{i,j+1} + \bar{h}_{i,j-0.5}^3 * \bar{p}_{i,j-1} - \left(\bar{h}_{i,j+0.5}^3 + \bar{h}_{i,j-0.5}^3\right) * \bar{p}_{i,j}}{(\Delta \bar{y})^2} \quad \text{.....................} \quad (19)$$

$$\frac{\partial \bar{h}}{\partial \bar{x}} = \frac{\bar{h}_{i+1,j} - \bar{h}_{i-1,j}}{2\Delta \bar{x}} \quad \text{...} \quad (20)$$

Equation 16-20 can be used in Equation 15 to get the desired result.

- ***The Pressure viscosity relation***

In this study, we incorporate an empirical relationship between viscosity and pressure, as formulated by Clarke et al. (2006).

$$\boldsymbol{\eta = \eta_0 exp\left\{\ln(\frac{\eta_0}{\kappa})\lfloor(1 + \chi p)^2 - 1\rfloor\right\}} \quad \text{......................................} \quad (21)$$

Where,

$\kappa = 63.15 x 10^{-6} Pa.s$

$\chi = 5.1 GPa^{-1} Pa.s$

$Z = \frac{\alpha_0}{\chi \ln(\frac{\eta_0}{\kappa})}$

- ***The Pressure density relation***

Per Dowson and Higginson[28] the relation is considered as below:

$$\boldsymbol{\rho = \rho(\rho) = \rho_0 \left(\frac{1 + \chi p}{1 + \lambda p}\right)} \quad \text{...} \quad (22)$$

Values of constant for the pressure coefficients are as below:

$$\boldsymbol{\gamma = 2.266\ Gpa^{-1}\ and\ \ \lambda = 1.683\ Gpa^{-1}}$$

1.6 Python Model Development In Line With Previous Topics

In this Novel method of calculation, the whole work process is divided in to 4 major steps such that it starts initially from the surface preparation, material assignment, and contact stress model deployment along with Lubricant model creation.

Fig. 3 Novel working methodology

- ***Surface Generation***

The RandomPerezSurface class method [23] is used to develop the surface with different surface finish condition. This method iterates between a surface with the required height function and another surface with the required Power Spectrum Density. With the iterations progress, these surfaces converge. This random surface requires us to set the height probability density function and the power spectral density of the output surface. Unlike the random filter method this method can only generate a single realisation of the random surface, further realisations require the optimisation problem to be solved again, with new random values. However, this method converges much more quickly than the filter method. Surface roughness significantly influences the friction, wear, and overall performance of machine parts. The Power Spectrum Density (PSD) serves as a key metric for characterizing surfaces from a tribological standpoint. Analytical models in contact mechanics utilize PSD to predict parameters such as contact area and stiffness, providing crucial

insights into the tribological properties of a surface. The Autocorrelation function [26], coupled with PSD, plays a pivotal role in this context [25]. In addressing the specific problem at hand, the surface finish is specified as 0.6Ra, and this characteristic is modeled using Python software, as depicted in Figure-4.,
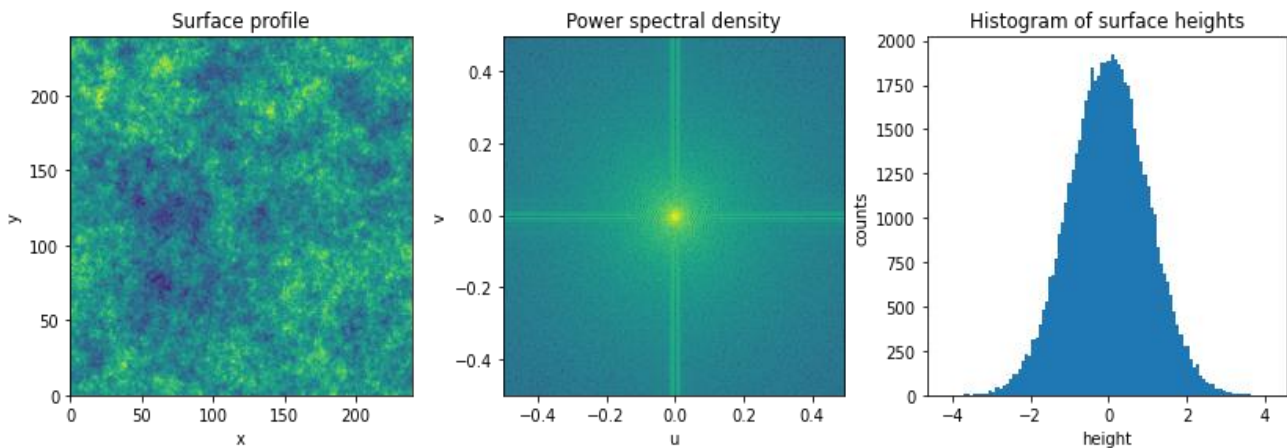

Fig. 4 Surface generation with profile, PSD and Histogram

As shown the surfaces almost perfectly fit the PSD, however the height function is well represented. Values of height are in micron and the histogram for the given sample shows that 95% of distribution is in between the value of -2-to-2-micron value. The limit for this value is +/- 6 Ra.

- *Contact Stress Model*

Once the surface is defined then the material is added and then contact model is generated. The contact model is generated in between the two idealised surface of contacting gear pair. For a contact model at least the first surface must be discretised (represented by a set of points). In this example the round surface is discretised while the flat surface is represented analytically Iterative method is used for the convergence of the load. To ensure the accuracy of result the numerical, analytical and error data is plotted in the figure 5. So accuracy of process is very high as error is near about 1%.
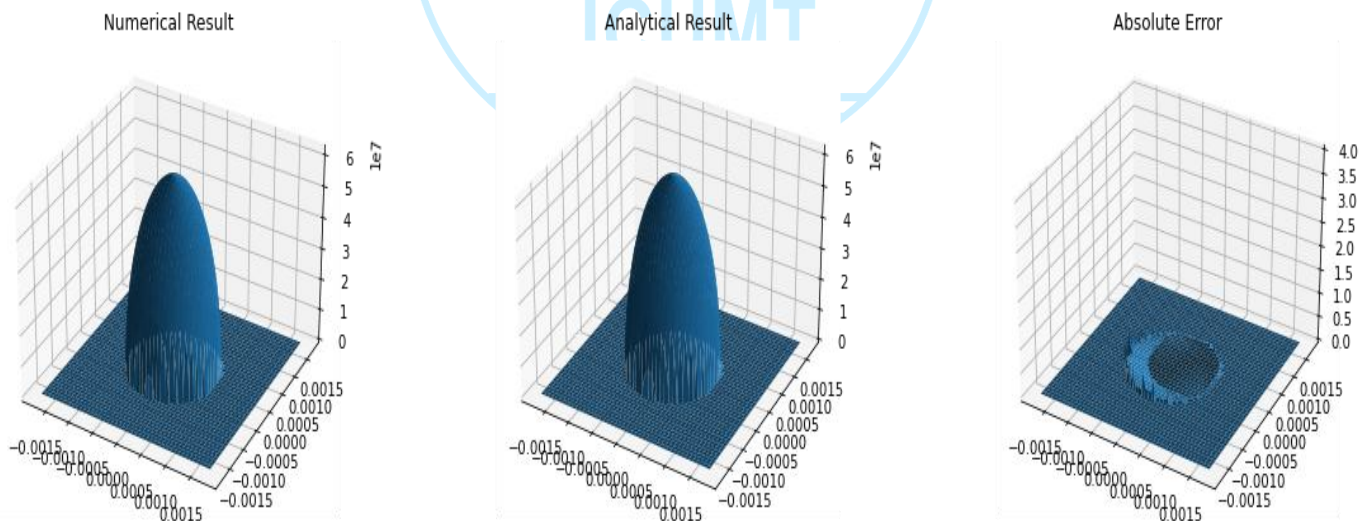
Fig. 5 Contact stress 3d generation for Numerical, Analytical and Absolute error value.

1.7 AGMA 925 Calculation

The AGMA 925 standard aligns with the recently issued Technical Report ISO/TR 15144-1 (2010). It is grounded in the Dowson and Higginson method and is formally expressed as an equation 23[25].

$$h_y = 1600\rho_{n,Y} * G_M^{0.6} * U_Y^{0.7} * W_Y^{-0.13} * S_{GF,Y}^{0.22} \quad \text{................................} \quad (23)$$

Material parameter value for the subject case is 3447.3. To perform the calculation of lubricant film thickness at 5 different points as calculates in section 1.3 we will use the detailed data of test gear pair which can be fed to Equation-23 per Kissling [25]. Various parameters calculated per kissoft are shown below.

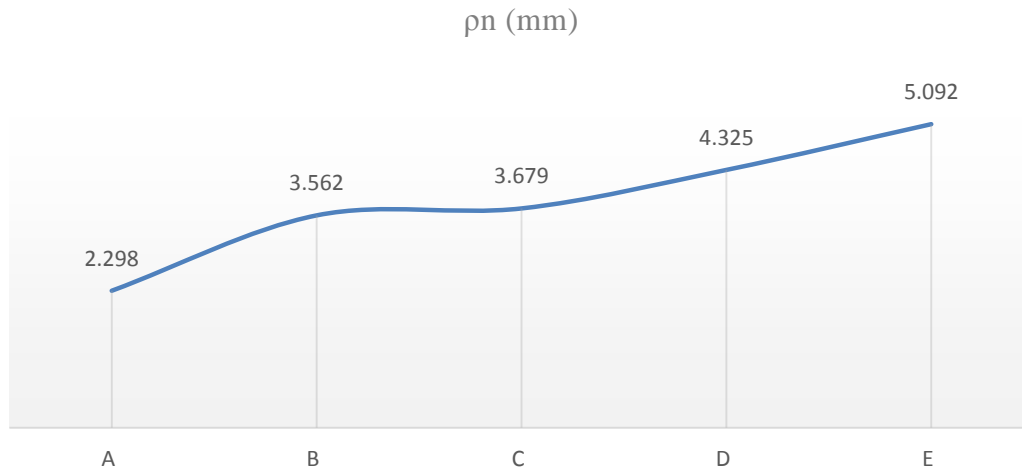- *Normal Relative radius of Curvature values are tabulated in Table 1*

ρn (mm)

Fig. 6 Variation of Relative radius of curvature over the Contact length.

Relative radius of curvature plays a critical role in the calculation as shown in Equation-23. It is clear from Figure-6 that its value is changing over the contact length starting from A to E. This is going to affect the lube film thickness calculation in the analytical as well as the noble method which is developed in python in earlier section. This will have impact on entraining velocities for sure. The detailed values and corresponding backup values is shown in Table 1.

Table 1 Relative Radius of Curvature Values

Index	ζ_j(rad)	d1 (mm)	ρ1 (mm)	ρ2 (mm)	ρn1 (mm)	ρn2 (mm)	ρn (mm)	Index
A	0.214	23.897	2.497	19.831	2.588	20.549	**2.298**	A
B	0.363	24.863	4.244	18.083	4.398	18.738	**3.562**	B
C	0.379	24.992	4.429	17.899	4.589	18.547	**3.679**	C
D	0.476	25.877	5.556	16.772	5.757	17.379	**4.325**	D
E	0.625	27.559	7.303	15.024	7.568	15.569	**5.092**	E

- *Specific Parameter values are tabulated in Table 2 as an output of kissoft Calculation.*

ve (m/s)
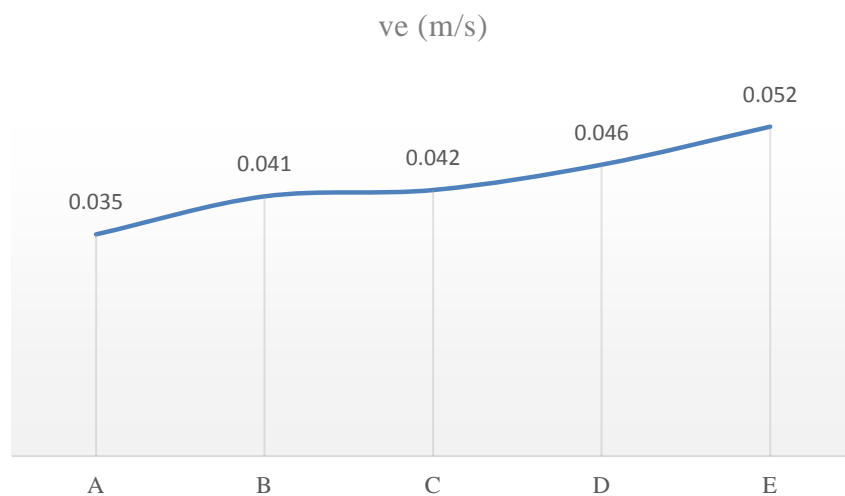
Fig. 7 Variation of entraining velocity over the Contact length.

As mentioned in relative radius of curvature section, entraining velocity is also going to get affected accordingly. It represents the velocity that draws oil between contacting gear teeth and increases EHL film thickness. It means that from point A to E the film thickness shall show some rise. Along with entrainment speed we need to consider the specific sliding parameter which is shown in Figure 8.
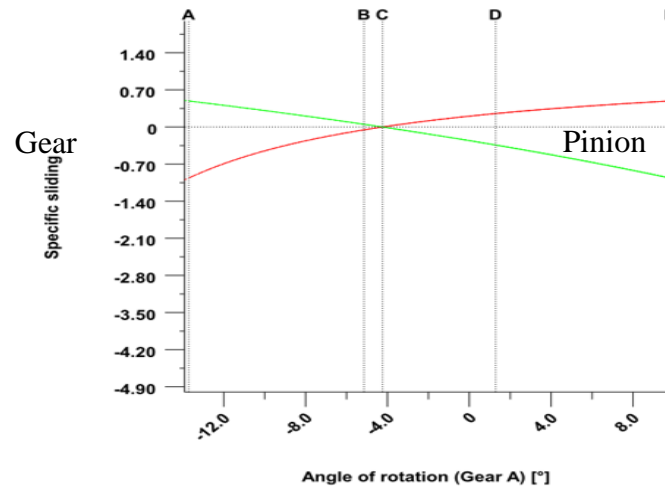
Fig. 8 Specific sliding of Gear and Pinion.

ζ_1: min = -0.964879, max = 0.491011, ζ_2: min = -0.964678, max = 0.491063

From Figure 8 the minimum and maximum value of specific sliding are same for both gear and pinion however point C is closer to point B on account of gear geometry. It means the point C to E will gave larger distance to travel and hence will be critical from oil thickness point of view. Table 2 gives the detailed parameter of speed related points:

Table 2 Speed Parameters

Index	ζ_j(rad)	d1 (mm)	vr1(m/s)	vr2(m/s)	vs (m/s)	ve (m/s)	vss1 (m/s)	vss2 (m/s)	Index
A	0.214	23.897	0.012	0.023	-0.011	0.035	-0.965	0.491	A
B	0.363	24.863	0.02	0.021	-0.001	0.041	-0.054	0.051	B
C	0.379	24.992	0.021	0.021	0	0.042	0	0	C
D	0.476	25.877	0.026	0.02	0.007	0.046	0.253	-0.339	D
E	0.625	27.559	0.034	0.018	0.017	0.052	0.491	-0.965	E

- *Specific film thickness distribution: It is important to understand the behavior of various parameter at the desired points to understand the lube film thickness distribution.*
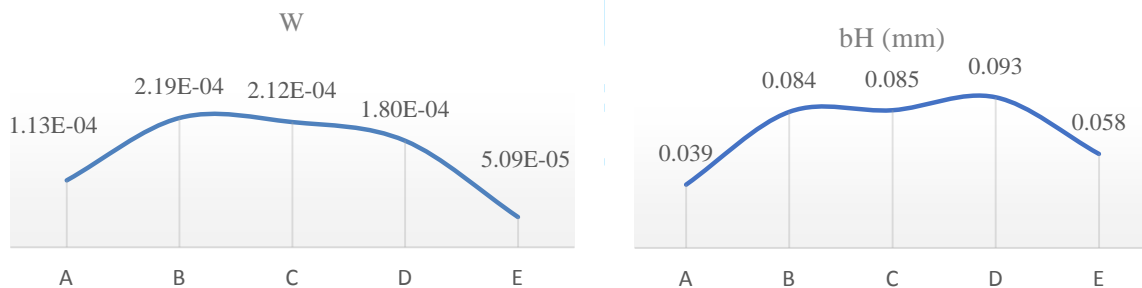
Fig. 9 Load Parameter (W) and Semi Width (bH) Variation.

Load parameter as shown in Figure 9 shows a rise and fall pattern. In between point B and C the pattern of curve is nearly similar where as it falls down. Contact point deflected dimension also shows nearly same pattern whereas the point D shows a change. This is happening as relative radius of curvature is increasing from point A to E. Ideally it should keep on increasing but the load sharing factor comes in picture which is shown in Figure 10.
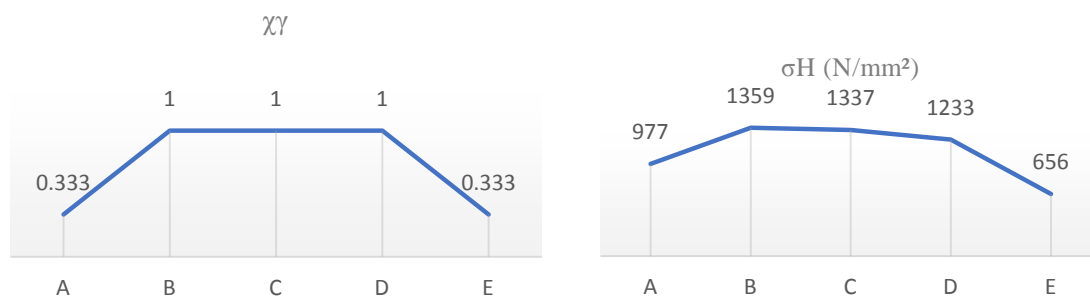

Fig. 10 Load Sharing Parameter($\chi\gamma$) and Contact Stress (σH) Variation

Load sharing parameter B to E shows A value of 1, which means one pair of tooth contact is there whereas the points A and E shows reduced value which shows that more than one pair of teeth are in contact. Similar pattern of load stress is also visible in contact stress distribution curve also.
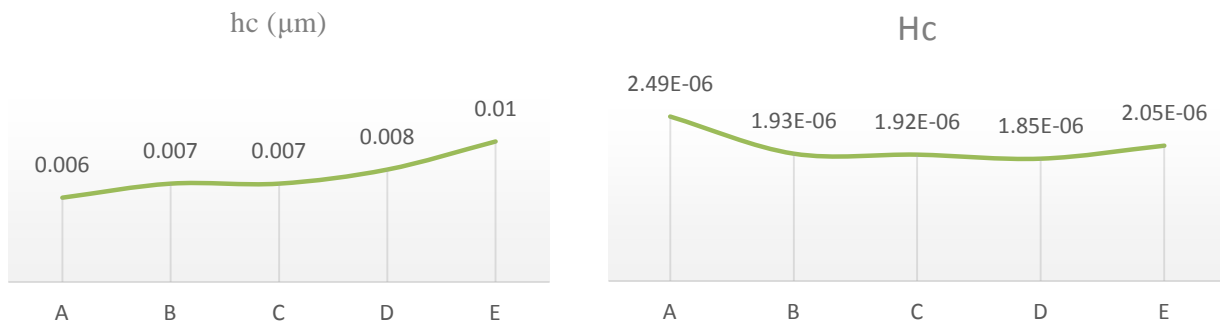

Fig. 11 Dimensional Lube film thickness (hc) and dimensionless form (Hc) variation.

Figure 11 shows the variation of Lube film thickness across all the points starting from Point A to E. Both dimensional and dimensionless form curves are drawn. Variation of these values are dependent on all the parameters like entraining velocity, Radius of curvature, load parameters and material parameter which includes the surface finish parameters as well. The consolidated values of all the discussed parameters are tabulated below in Table 3.

Table 3 Parameters affecting film thickness

Index	χγ	σH (N/mm²)	U	W	Hc	hc (μm)	bH (mm)	λ2bH
A	0.333	977	5.40E-13	1.13E-04	2.49E-06	0.006	0.039	0.022
B	1	1359	4.10E-13	2.19E-04	1.93E-06	0.007	0.084	0.018
C	1	1337	4.03E-13	2.12E-04	1.92E-06	0.007	0.085	0.018
D	1	1233	3.76E-13	1.80E-04	1.85E-06	0.008	0.093	0.02
E	0.333	656	3.63E-13	5.09E-05	2.05E-06	0.01	0.058	0.032

Load sharing factor distribution from point A to E shows the condition of uniform meshing [25]. Values of contact stresses are rounded to avoid decimal points; however, the values are not exactly same and is reducing even for load sharing factor value 1. The reason for this is driven by helix angle factor, radius of curvature, contact stress factor and some other small points which are not in the scope of this research work so not discussed in detail. Speed parameter (U) shows a slight reduction in the value however will be more in the next section where the EHL model will show its effect on lube film pressure. Load parameter is showing a reducing value from A to e as it is affected by relative radius of curvature value of the corresponding point and this value is in denominator of the calculation causing its reduction over points. Semi width (bH) is directly proportional to the load sharing factor and relative radius of curvature and hence it is following the similar pattern over points A to E.

1.8 Output of Python Program-Noble Method of Calculation

For the Considered problem statement various parameters required at five critical points were considered and the lube pressure and lube film thickness is plotted at each point. Last figure of each Figure is having green border to visualize the difference between each point Figure value,
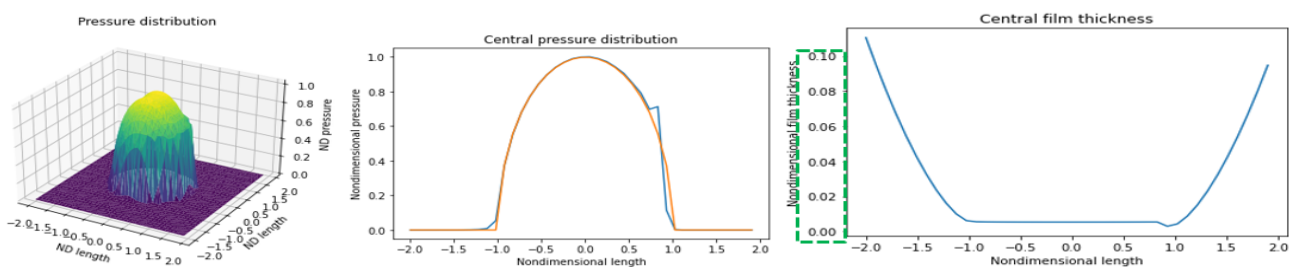
- *At Point-A*

Fig. 12 Lubricant Pressure and Lube film thickness pattern at Point A.

Point A is the start of contact on the gear pair where the load is not maximum and is shared by at least two gear pair such that the load is distributed to the contact point by 33%. The direction of oil film entrance is from the side opposite to the spike seen in the middle of the Figure 12. The first figure shows the 3d view of the stress distribution on non-dimensional coordinates and it covers both contact pressure as well as hydrodynamic pressure. Oil entraining velocity is very low at

this point and the geometry of deflection is smallest. The hydrodynamic pressure follows the contact pressure curve exactly same expect at the exit there is pressure spike which is expected. The non-dimensional lube film thickness show the at that before the contact point A the lube oil is in abundance and hence no issue of thickness there where as at the point A from entrance to exit which is shown by the length -1 to 1 lube film thickness has gone down but higher than 0 value. Dimensionally it is in micron value.

- *At Point-B*
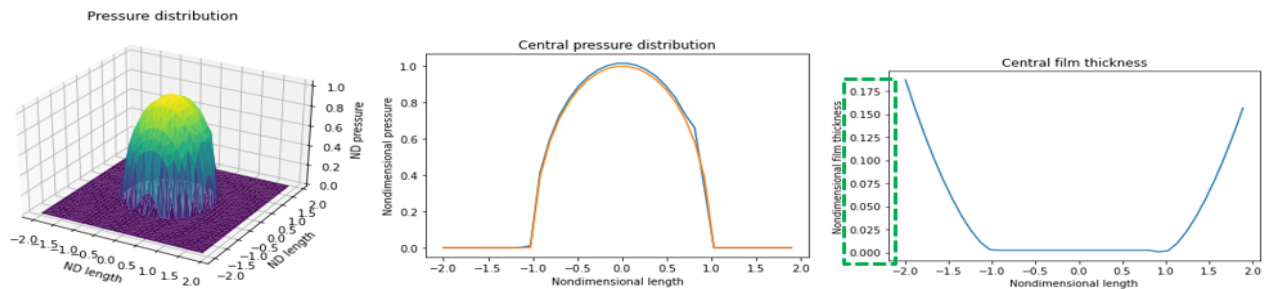
Fig. 13 Lubricant Pressure and Lube film thickness pattern at Point B.

Point B represents the next critical contact point. Since the tooth is not having any modification an d looks like it is not so kinematically designed the load sharing at this point is coming as 100% which usually comes 75% in regular design. However, there is no major concern with this and it is quite possible [25]. Since the point load at this point is maximum possible so the deformation geometry is also on higher side as discussed as shown in earlier section. As we are moving from point A to B the radius of curvature is also changing and is in positive side which is affecting the oil entraining velocity. Since the load is high and the deflected zone have dimensions in both axes but being one dimension on higher side other is ignored in the calculation. The other ignored small dimensions is becoming the potential leakage issue of the oil and hence at the oil discharge end of the contact point the pressure spike is not so high. The first figure shows the 3d view of the stress distribution on non-dimensional coordinates and it covers both contact pressure as well as hydrodynamic pressure. Oil entraining velocity is higher as compared to point A at this point and the geometry of deflection. The hydrodynamic pressure follows the contact pressure curve exactly same expect at the exit there is small pressure spike (reason discussed earlier) which is expected. The non-dimensional lube film thickness shows the at that before the contact point B the lube oil is in abundance and hence no issue of thickness which means there is considerable gap between A and B points.
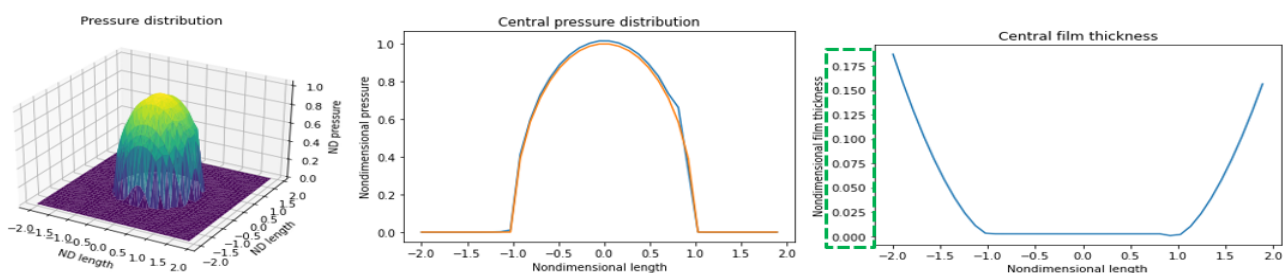
- *At Point-C*

Fig. 14 Lubricant Pressure and Lube film thickness pattern at Point C.

Point B and C are very closed to each other as per the calculation performed in section 1.3. Similar explanation of point B is applicable here as well.
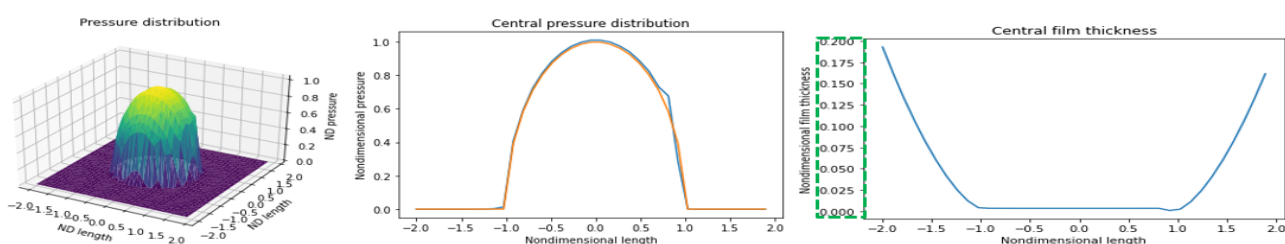
- *At Point-D*

Fig. 15 Lubricant Pressure and Lube film thickness pattern at Point D.

Point D is the second last point of contact on the gear pair where the load is maximum per section 1.7. The direction of oil film entrance is from the side opposite to the spike seen in the middle of the Figure 15. The reason of not getting the higher spike is same as explained about Point B. The first figure shows the 3d view of the stress distribution on non-dimensional coordinates and it covers both contact pressure as well as hydrodynamic pressure. Oil entraining velocity is higher at this point and so the geometry of deflection as compared to point C. The nature of curve looks similar to point C but the difference can be easily visible in the last figure where the vertical axes values are different.
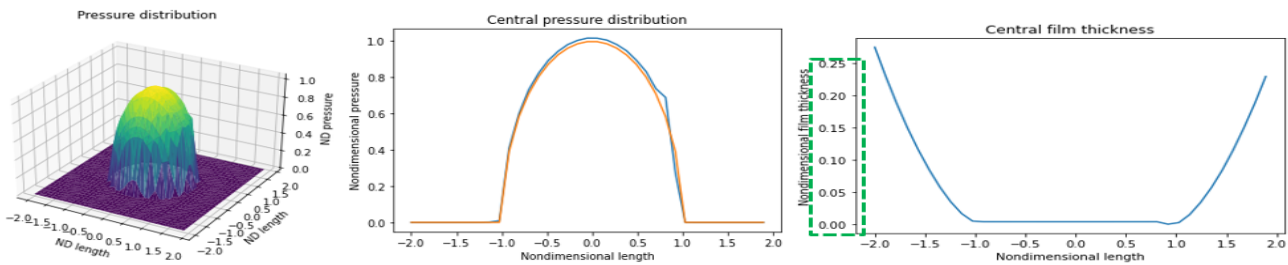
- *At Point-E*

Fig. 16 Lubricant Pressure and Lube film thickness pattern at Point E.

Point E is the last point of contact on the gear pair where the load is not maximum and is shared by at least two gear pair such that the load is distributed to the contact point by 33%. The direction of oil film entrance is from the side opposite to the spike seen in the middle of the Figure 16. The first figure shows the 3d view of the stress distribution on non-dimensional coordinates and it covers both contact pressure as well as hydrodynamic pressure. Oil entraining velocity is very high at this point and the geometry of deflection is smallest. The hydrodynamic pressure follows the contact pressure curve exactly same expect at the exit there is pressure spike which is expected. The nature of curve is bit different but overall, the values are different as can be clearly seen from the lube film thickness curve image at last.

The whole discussion from point A to E was for about 7 mm and even in this the load, speed, and other geometric parameters were varying. It was difficult to get a visible significance change from the five curves, but the lube film thickness data provides good comparison and varying film thickness at different point. This pattern is also inline with section 1.7 finding.

2. Comparison of The Newmethod Result With Historic Data

It is important to ensure the accuracy of the output of Noble method with historic proven data. To have this comparison the famous work of Dowson & Higginson [28] is considered to compare with the output of noble method. Figure 17 shows the Pressure distribution of oil film in contact zone. the curves are denoted by numbering starting from 0 to 6. The curve with named 0 is for dry friction. Thus, there is no lubricant, and it will behave as contact stress zone as a hemisphere.
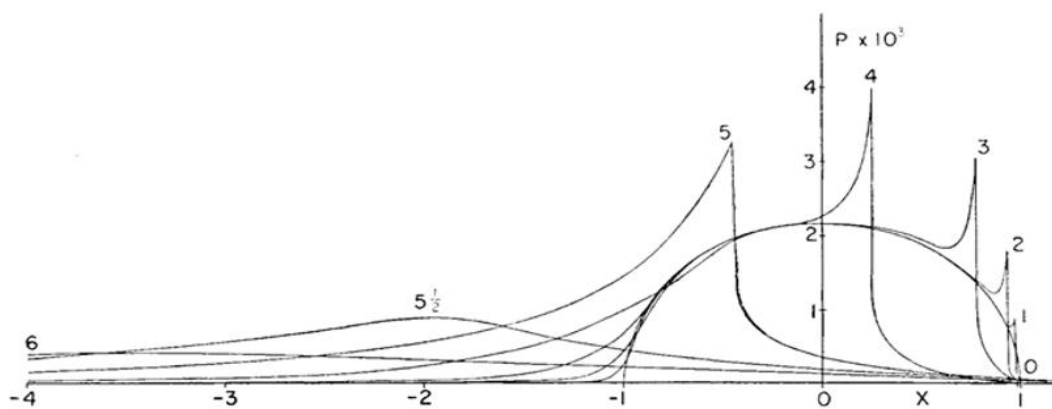

Fig. 17 Pressure results for EHL Line contact for varying speed [28].

All Curve with 1 value is applicable for U parameter in the range of 10^{-13}, and its power is getting reduced from curve 2 to 6 with minimum U parameter value as 10^{-8}. All these curved were prepared for the constant material parameter value G is 5000, weight parameter W as 3 x 10^{-5}.On a similar value the graphs were produced with the new tool developed during this research work and for clarity the curved were produced separately as shown below:
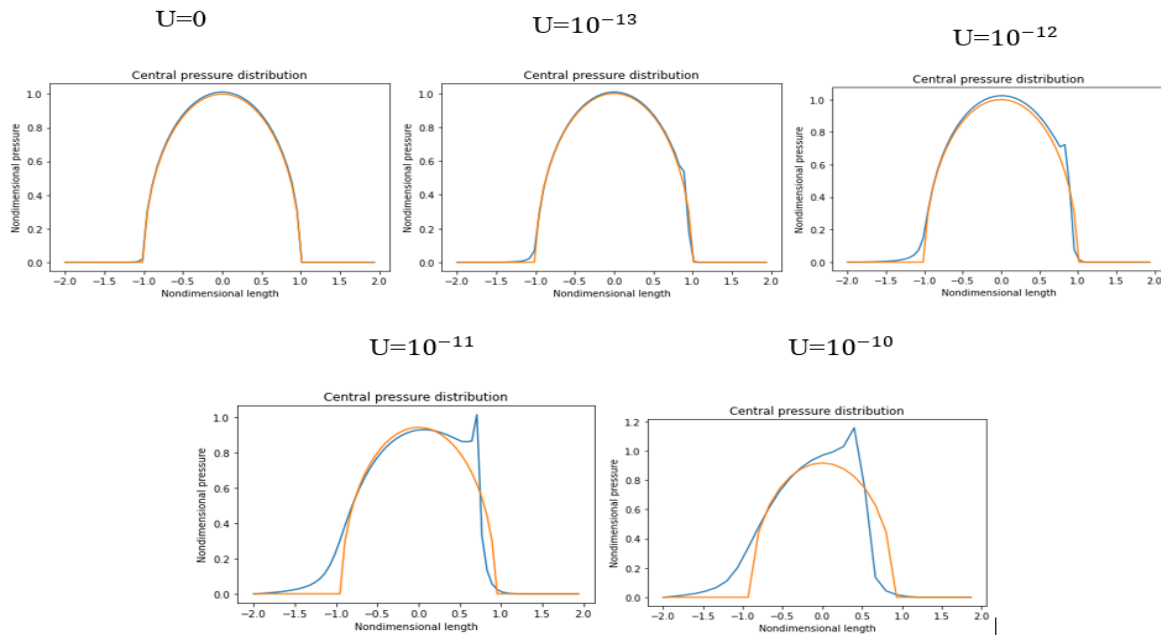
$$U=0 \qquad U=10^{-13} \qquad U=10^{-12}$$

$$U=10^{-11} \qquad U=10^{-10}$$

Fig. 18 Pressure results for EHL for varying speed.

Figure 18 shows the scaled version of the results of EHL output model from the new tool developed in this resaerach. To save the calculation time the no of panels were considered 63 which was not known for the values considered by Dowson et al.[28]. Overall the pattern looks promisingly same and the comparable with respect to AGMA standard also.

3. Discussion of the Results

➢ Python software was used to develop the new EHL model calculation tool. Various references as cited were considered to develop the tool to calculate the EHL model. Idea after this development was to develop a low-cost tool which can be used without Matlab or other softwares. Because of data privacy limited and required details were shared in this research work.

➢ AGMA-925 is globally recognized technical document for calculating the lube fim thickness and necessary geometry of the gear pair. A detailed analysis with the help of this technical document was done at all the respective point. Speed parameter was the most driving parameter for the lube film thickness was found.

➢ Specific sliding curve gave a detailed vision of how sliding speed is affecting the specific sliding ratio and the extreme values as shown in the Figure8. This curve also has given the distribution of sliding along the contact line at different desired point alongwith the internal distances.

➢ New developed tool output was compared with past historic data and a good agreement was found, however due to scale and local resource constrained these were not identical to each other. But the pattern was similar which shows that the results of new tool can be used inline.

➢ Detail analysis of each point with respect to the new tool was found in line with AGMA comments and need also. Overall the new tool has given detailed vision at each critical point on the contact line. The output can be used to understand the pressure spike of oil at each point and the reason for this which is directly related to the geometry of deflection there.

4. Conclusion and Future Scope

The semi approach method which was used in this research was found useful for small sizes whereas based on the research experience the system processing would be required on higher end to compute to many iterations. Speed parameter which is resulting in oil entraining velocity change is the critical parameter for determining the lubrication condition at a point. A speed is low then the time at each point would be more and parallels the time required for oil to escape the contact point would be more which can deteriorate the contact point zone on account of oil scarcity. A good future scope with this method would be to calculate the oil loss during meshing process from the respective contact point.

References

[1] Hugh Spikes, Zhang Jie, "History, Origins and Predictions of Elastohydrodynamic Friction," *Tribology*, vol. 56, pp. 1–25, Aug-2014.

[2] G E Morales, A W Wemekamp, "Ertel-Grubin methods in Elastohydrodynamic lubrication-a review," *Journal of Engineering Tribology*, pp. 15–34, Oct-2008.

[3]   D. Dowson, B. J. Hamrock, "Isothermal Elastohydrodynamic Lubrication Point Contact Part-I," *Journal of Lubrication Technology*, pp. 223-228, Apr-1976

[4]   T G Huges, C D Elcote, H P Evans, "On the Coupling of the elastohydrodynamic problem," *Process Institution Mechanical Engineers*, vol. 2012, part c, Oct 1997.

[5]   T G Huges, C D Elcote, H P Evans, "Coupled solution of the elastohydrodynamic line contact using a differential deflection method," *Process Institution Mechanical Engineers*, vol. 2014, part C, APRIL 1999.

[6]   H P Evans, R.W. Snidle, "The isothermal elstohydrodynamic Lubrication of spheres",Journal of Lubrication Technology, vol. 103, pp. 547–557, Oct. 1981.

[7]   H P Evans, T G Hughes, "Evaluation of deflection of Sem infinite bodies by differential method," *Process Institution Mechanical Engineers*, vol. 214, Jun . 2015.

[8]   Lin Han,Da-Wei Zhang, Fu-Jun Wang, "Predicting film parameter and friction coefficient of helical gears considering surface roughness and load variation," *Tribology*, vol. 56, no. 1, pp. 49-57, Jan. 2013.

[9]   M. Kaneta, A. Cameron, "Effect of Asperities in Elastohydrodynamic Lubrication," *Tribology*, vol. 102, pp. 374–378, Jul 1980.

[10]   S. Li, A. Kahraman, "A transient mixed elastohydrodynamic lubrication step for spur gear pairs," *Journal of Tribology*, vol. 132, Jan. 2010.

[11]   G. Nijenbanning, C.H. Venner, H. Moes, "Film thickness in elastohydrodynamically lubricated elliptic contacts,*" Journal of Wear*, vol. 176, pp. 217–229, Mar. 1994.

[12]   A. P. Ranger, "The solution of the Point contact Elasto-Hydrodynamic Problem," *International Journal of Royal Society*, vol. 346, pp. 227–244, 1975.

[13]   R.J. Chittenden, D. Dowson, j. f. Dunn, C. M. Taylor, "A theoretical analysis of isothermal elastohydrodynamic lubrication of concentrated contacts," *Journal of Royal Society*, vol. 397, pp. 245–269, 1985.

[14]   Xiaolan Ai, Herbert S. Cheng, "A transient EHL analysis for line contacts with measured surface roughness using multigrid technique," *Journal Of Tribology*, vol. 116, pp. 549–556, Jul. 1994.

[15]   Xiaojing Wang, Yang Dong, Jingjing zhang, Bal Dan "On the Relationship between Micropitting and Friction/Wear of Rolling-Sliding Steel/Steel Contacts," ACM Journal, pp. 64–71, July 2022.

[16]   Olson Robin, Mark Michaud, Keller Jonathan "A Case study of ISO/TS 6336-22 Micropitting calculation," Journal of Gear technology, vol. 11, pp. 48–57, April. 2021.

[17]   Xiangyang Xu, Yinghua Liang, Zhu Wang "A Novel tooth relief method for reducing micro-pitting of spur gears," ACM Journal, pp. 1–34, April 2022.

[18]   A.C. Redlich, D Bartel, H Schorr, L Deters "A Deterministic EHL Step for Point Contacts in Mixed Lubrication Regime," Thinning Films and Tribological Interfaces, 2000 pp. 85-93,

[19]   C.E. Goodyer,R. Fairlie, M. Berzins, L.E. Scales "An In depth Investigation of the Multigrid Approach to Steady and Transient EHL Problems" Thinning Films and Tribological Interfaces, vol 38, pp. 95-102,2000.

[20]   Alexei Jolkin, Roland Larsson "Determination of Lubricant compressibility in EHL conjunctions using the Hybrid technique" Thinning Films and Tribological Interfaces, vol 38, pp. 589-596,2000.

[21]   Shahram Khalilarya, Iraj Mirzaee, Mahdi Mohammadpour, Davoot Jalali Vahid "A numerical step to calculate Elastohydrodynamic (EHL) properties in involute spur gears" International conference on Mechanical and Electrical Technology (ICMET 2010)

[22]   Keying Chen, Liangcai Zeng, Juan Chen, Xianzhong Ding "Analysis of line Contact with the particles under rougfh contact surface" Advances in Material science and Engineering, Volume 2020.

[23]   K.K. Manesh,B. Ramamoorthy, M. Singaperumal "Numerical generation of anisotropic 3D non-Gaussian engineering surfaces with specified 3D surface roughness parameters",Journal of Wear,Volume 268,pp: 1371-1379, May-2010.

[24]   Francesc Pérez-Ràfols, Andreas Almqvist "Generating randomly rough surfaces with given height probability distribution and power spectrum",Journal of Wear,Volume 131,pp: 591-604, Mar-2019.

[25]   Ulrich Kisling, "Application of the First international calculation method of Micropitting", Gear technology, pp:54-60,May-2012.

[26]   Pawel Pawlus, Rafal Reizer, Michal Wieczorowski, "A Review of the method of random surface topography modeling", Tribology International, Vol-152, pp:1-23,Jul-2020

[27]   Dongri Liao, Wen Shao, Jinyuan Tang, Jianping Li , "An improved rough surface modeling method based on linear transformation technique", Tribology International, Vol-119, pp:786-794, Mar-2018

[28]   D. Dowson, G. R. Higginson, "Elastohydrodynamic Lubrication," *Pergamon press limited*, pp. 78-105, Apr-1977

[29]   Quentin Allen, Bart Raeymaekers, "Soft EHL Simulations of Lubricant Film Thickness in Textured Hard-on-Soft Bearings Considering Different Cavitation Models, in the Context of Prosthetic Hip Implants", Tribology, pp. 1-17, Aug-2021

[30] MG Wu, XZ Hu, "Elastohydrodynamic lubrication analysis of spur gear under mixed friction condition",Journal of Physics, pp: 1-6, 2022.

[31] Quentin Allen, Bart Raeymaekers, "Convergence of (Soft) Elastohydrodynamic Lubrication Simulations of Textured Slider Bearings", Lubricants, pp:1-18, Feb-2023.

[32] Ferdinand Schmid, Constantin Paschold, Thomas Lohner, Karsten Stahl, "Characteristics in hard conformal EHL line contacts", Industrial Lubrication and Tribology, pp: 730-740, Nov-2023.

[33] Yangyi Xiao, Mengjie Zou, Wankai Shi, Minglin Kang, "Analysis of the Surface/Interface Damage Evolution Behavior of a Coating–Substrate System under Heavy-Load Elastohydrodynamic Lubrication", Journal of Coating, pp:1-14, Sept.-2019.

[34] Yuko Higashitani, Sanemasa Kawabata, Marcus Bjorling, Andreas Almqvist, "A traction coefficient formula for EHL line contacts operating in the linear isothermal region", Tribology, pp:1-8, Jan-2023.

[35] Chunxing Gu, Di Zhang, Xiaohui Jiang, Xianghui Meng, Shuwen Wang, Pengfei Ju, Jingzhou Liu, " Mixed EHL Problems: An Efficient Solution to the Fluid–Solid Coupling Problem with Consideration of Elastic Deformation and Cavitation" , Lubricants, pp: 1-17, Nov-2022.

[36] Zhaoqiang Wang, Bo Han, Lingtao Sun, "Analysis of Elastohydrodynamic Lubrication (EHL) Characteristics of Port Plate Pair of a Piston Pump", Machines, pp: 1-25, Nov.-2022.

[37] Hai Chao Liu, Bin Bin Zhang, Volker Schneider,, C.H. Venner, G. Poll, "Two-dimensional generalized non-Newtonian EHL lubrication: Shear rate-based solution versus shear stress-based solution", Journal of engineering Tribology, pp:2626-2639,Sept. 2021.